# Photovoltaic application of the V, Cr and Mn-doped cadmium thioindate

C. Tablero

A B S T R A C T

The $CdIn_2S_4$ spinel semiconductor is a potential photovoltaic material due to its energy band gap and absorption properties. These optoelectronic properties can be potentiality improved by the insertion of intermediate states into the energy bandgap. We explore this possibility using M = Cr, V and Mn as an impurity. We analyze with first-principles almost all substitutions of the host atoms by M at the octahedral and tetrahedral sites in the normal and inverse spinel structures. In almost all cases, the impurities introduce deeper bands into the host energy bandgap. Depending on the site substitution, these bands are full, empty or partially-full. It increases the number of possible inter-band transitions and the possible applications in optoelectronic devices. The contribution of the impurity states to these bands and the substitutional energies indicate that these impurities are energetically favorable for some sites in the host spinel. The absorption coefficients in the independent-particle approximation show that these deeper bands open additional photon absorption channels. It could therefore increase the solar-light absorption with respect to the host.

## 1. Introduction

Ternary semiconductor materials have attracted attention for a wide range of potential applications in device technology because of the presence of three different chemical components, which could allow the tailoring of some of the physical properties. Among these compounds, spinels comprise an important class of ceramic compounds with a variety of interesting physical properties.

The general formula for an spinel is $(A_{1-x}B_x)[A_xB_{2-x}]X_4$ ($0 \leqslant x \leqslant 1$), where A and B represent differently cations, X is an anion, the square brackets (parenthesis) correspond to the octahedral (tetrahedral) sites, and $x$ represents the degree of inversion. The two end-members are normal spinel ($x = 0$, $(A)[B_2]X_4$) and inverse spinel ($x = 1$, $(B)[AB]X_4$). In a normal spinel, the A atom has four nearest-neighbor X atoms, while the B atom is in the corner of the octahedron cluster with six nearest-neighbor X atoms. The X atoms have one A atom and three B atoms as their nearest neighbors. In an inverse spinel structure, the tetrahedral sites are occupied by B atoms while the octahedral sites are occupied by equal numbers of A and B atoms. In many spinels the degree of inversion varies with temperature [1]. At high temperatures, spinels tend toward the random distribution $x = 0.66$. A diversity of cations of different size and charge may enter the *spinel* structure. Spinels are classified by cation oxidation state, where A is 2+, 4+, or 6+ and B is 3+, 2+, or 1+. The two most common spinel types are 2–3 (the spinel contains 2+ and 3+ cations) and 4–2 spinels.

Among the ternary 2–3 spinels, the magnesium and cadmium indium sulfide are currently used for optoelectronic application as photoconductors. In particular, the $CdIn_2S_4$ spinel semiconductor is an attractive material with a potential capability for applications in luminescence [2], photoelectronics [3], X ray dosimetric property photoconductors [4], solar cells, and light emitting diodes (LED) [5–9].

The optoelectronic properties of these spinels can be potentiality improved by the insertion of intermediate states into the energy bandgap. For example, because their energy band gaps lie in the region of optimum gaps for the implementation of an intermediate-band (IB) material [10], they are also considered as promising candidate for photon absorbing materials for IB solar cells.

From the previous comments, it is opportune to analyze whether the insertion of intermediate states into the energy bandgap using selected impurities improves the electro-optical properties of the host spinel for device applications. In this work, we shall present a detailed theoretical study of the doped-$CdIn_2S_4$ ternary spinel compound. We will try to explore the resulting electronic properties in order to apply these materials to optoelectronic devices. We analyze the V, Cr and Mn as possible dopants because they introduce intermediate states into the energy bandgap. The occupation of these states, depending on the site and the atom substitution, is different. They are empty, partially full or full. All possible substitutions of the Cd and In atoms by these impurities in the normal and the inverse structures are considered. Attention is also paid to the contribution of the impurity states to the final intermediate states, and to the relative stability.

## 2. Calculations

In order to obtain the total energies we carried out spin polarized calculations with periodic boundary conditions. Computations, based on the density-functional theory (DFT) [11] in the generalized gradient approximation (GGA), have been carried out for the two possible substitutions in the normal structure: $(Cd_{1-y}M_y)[In_2]S_4$ and $(Cd)[In_{2-y}M_y]S_4$; and the three in the inverse: $(In)[Cd_{1-y}M_yIn]S_4$, $(In_{1-y}M_y)[CdIn]S_4$, $(In)[CdIn_{1-y}M_y]S_4$. The supercells used for all cases containing 112 atomic sites ($y = 0.0625$).

The standard Kohn–Sham [12] equations are solved self-consistently [13]. For the exchange and correlation term, the GGA in the form of Perdew et al. [14] has been used. The standard Troullier–Martins [15] pseudopotential is adopted and expressed in the Kleinman–Bylander [16] factorization. The Kohn–Sham orbitals are represented using a linear combination of confined pseudo-atomic orbitals [17]. An analysis of the basis set convergence (with both size and the confinement potential of the orbitals) has been carried out using from single-zeta to double-zeta with polarization basis sets for all atoms and varying the number of the special $k$ points in the irreducible Brillouin zone. In all of the results presented in this work a double-zeta with polarization functions basis set has been used with periodic boundary conditions and 18 special $k$ points in the irreducible Brillouin zone for a 112-atom cell.- From the imaginary part of the dielectric function $e_2$ is possible to obtain the others optical functions, as for example the absorption coefficient. $e_2$ is directly related to the electronic band structure, in particular to the energies ($E_{\mu,\vec{k}}$) and the occupations ($f_{\mu,\vec{k}}$) of the $\mu$ bands. It can be computed by summing up all possible transitions from the occupied to the unoccupied states, taking into account the appropriate transition dipole matrix elements $p_{\mu\lambda} = <\mu,\vec{k}|\hat{p}|\lambda,\vec{k}>$ between the states $|\mu,\vec{k}>$ and $|\lambda,\vec{k}>$ of the $\mu$ and the $\lambda$ bands at point $\vec{k}$ of the Brillouin zone:

$$e_2(E) \sim \frac{1}{E^2}\int \frac{d\mathbf{k}}{(2\pi)^3}\sum_{\mu}\sum_{\lambda}|p_{\mu\lambda}|^2[f_{\mu,\vec{k}} - f_{\lambda,\vec{k}}]\delta(E_{\lambda,\vec{k}} - E_{\mu,\vec{k}} - E)$$

## 3. Results and discussion

The primitive $CdIn_2S_4$ unit cell of the spinel lattice contains 2 formula units and has a lattice constant of $a = 10.797$ Å [18–20], where the anion displacement parameter $u$ is 0.386. It is generally accepted that $CdIn_2S_4$ crystallizes into a normal spinel structure. Nevertheless, studies involving partial inverse structures and mixed crystals have also been reported [21].

There is general agreement that the bandgap of $CdIn_2S_4$ is indirect [19,22–26] and that the valence band (VB) maximum is not at the $\Gamma$ ($k = 0$) point but probably in the [1 1 0] direction [25,26]. A detailed study of the gap energy and of the direct or indirect character of the energy bandgap with the anion displacement parameter $u$ has been done in reference [26]. We use the parameters in reference [26] for all supercells. With these parameters and the same methodology, the results for the electronic and optical properties compare well with experimental and other data in the literature [26].

When a host atom, Cd or In, is substituted by an impurity M in the general spinel $(Cd_{1-x}In_x)[Cd_xIn_{2-x}]S_4$ ($0 \leqslant x \leqslant 1$) there are two possibilities: that the impurity atom occupies a tetrahedral or an octahedral site. For the two end-members, normal ($x = 0$) and inverse ($x = 1$) these possibilities are lower than for an arbitrary $x$. For the $M_{Cd}$ substitution in the normal and inverse spinel the possibilities are $(Cd_{1-y}M_y)[In_2]S_4$ for the normal and $(In)[Cd_{1-y}M_yIn]S_4$ for the inverse structure respectively. In both cases, the M impurity atom occupies a tetrahedral site. The $y$ index indicates the impurity concentration. For the $M_{In}$ substitution, the M atom occupies a tetrahedral site in the normal structure, i.e. $(Cd)[In_{2-y}M_y]S_4$, whereas it can occupy both tetrahedral and octahedral sites in the inverse structure: $(In_{1-y}M_y)[CdIn]S_4$ and $(In)[CdIn_{1-y}M_y]S_4$.

Using the nomenclature of square brackets and parenthesis to indicate the octahedral and tetrahedral sites, and a subindex to specify the structure, the possible substitutions are: $[M_{In}]_{x=0}$, $(M_{Cd})_{x=0}$, $[M_{In}]_{x=1}$, $(M_{In})_{x=1}$, and $[M_{Cd}]_{x=1}$, with M = V, Cr and Mn. The band structure is shown in Figs. 1–3 (panels a–e). In these figures only the majority spin component that presents the IB is shown. The band structures for the minority spin components are similar both between themselves, and similar to the band structure of the host semiconductor. For the inverse substitutions the energy bangap is lower than for the normal structure. In many of the substitutions the doped spinels have states in the energy bandgap. Particularly interesting cases are the $(Cr_{Cd})_{x=0}$, $(V_{Cd})_{x=0}$, and $[Mn_{In}]_{x=0}$ substitutions with a partially-full IB isolated from the VB and the conduction band (CB) (The IB has been shadowed in the Figures). Other cases are: $(Cr_{In})_{x=1}$ and $[Cr_{Cd}]_{x=1}$ substitutions, where there is a partially-full band that overlaps with the VB and CB respectively; $[Cr_{In}]_{x=0}$, $[Cr_{In}]_{x=1}$, $[V_{In}]_{x=0}$, $[V_{In}]_{x=1}$, and $(V_{In})_{x=1}$ substitutions, where there are empty IB above the Fermi energy.

In the previous cases, in addition to the VB-CB host semiconductor transition, there are other possible transitions. It depends on the occupation of the IB. If the IB is full or empty the additional transitions with respect to the host semiconductor can be IB-CB and VB-IB respectively. When the IB is partially full these two transitions can happen simultaneously. The latter situation generates additional carriers (electrons in the CB and holes in the VB) increasing the current that can be extracted, and thus, raising the efficiency to absorb the solar radiation of these solar cell devices.

The symmetry of the IB bands depends on the substitution type. When the impurity atom occupies an octahedral site, it has six nearest-neighbor S atoms, whereas if it occupies a tetrahedral site has four nearest-neighbor S atoms. For example, in the normal $CdIn_2S_4$ structure, the In atom has six nearest-neighbor S atoms at 2.58 Å, the Cd atom is surrounded by 4S at 2.54 Å, and the S atom is bounded by 1Cd (2.54 Å) and 3In (2.58 Å). This local symmetry effect determines the character of the IB in the bandgap.

The fivefold degenerated $d$-states of the impurity are split by the crystalline field at the substitutional sites into $d_e$-states ($d_{z^2}$ and $d_{x^2-y^2}$) and $d_t$-states ($d_{xy}$, $d_{xz}$, and $d_{yz}$). The $t$-IB states with $t$ symmetry are formed mainly by the combination of the $d_t$ states of the impurity atoms and by the neighboring $p$-S nearest-neighbor (six and four at octahedral and tetrahedral sites respectively) states with $t$ symmetry ($H_t$): $t \sim \alpha_t \cdot d_t + \beta_t \cdot H_t$. Similarly, for the $e$-IB states, $e \sim \alpha_e \cdot d_e + \beta_e \cdot H_e$. In addition, the spin splits these groups. In general, $\beta_e$ is very small and the $e$ states remain as non-bonding impurity states. On the other hand, if $\beta_t$ is appreciable and the partner of the $t$-IB (anti-bonding component) is in the VB (bonding component), the implications with respect to the non-radiative recombination could be important [27]. In this case, the charge density around the impurity is equilibrated in response to the perturbations in the equilibrium nuclear configuration and the charge of the intermediate band [27] reducing the non-radiative recombination. This equilibration is through the modification of the contribution from the impurity to the IB and to the VB band.

In order to analyze this splitting and the orbital contribution of $d$-impurity states to the IB, we have carried out a projected density of states (DOS) for the majority spin components shown in Figs. 1–3 (panels f–j). When the local site symmetry is tetrahedral (octahedral) the $d$-impurity states that contribute to the IB in the energy band gap are the $d_t$-states ($d_e$-states). Because the local symmetry around of the impurity is slightly distorted with respect to the tetrahedral and octahedral, the contribution of the two $d_e$-states or of the three $d_t$-states is different depending on the substitution. For example, this is clearly illustrated for the $[Cr_{In}]_{x=1}$ and $(V_{In})_{x=1}$. This

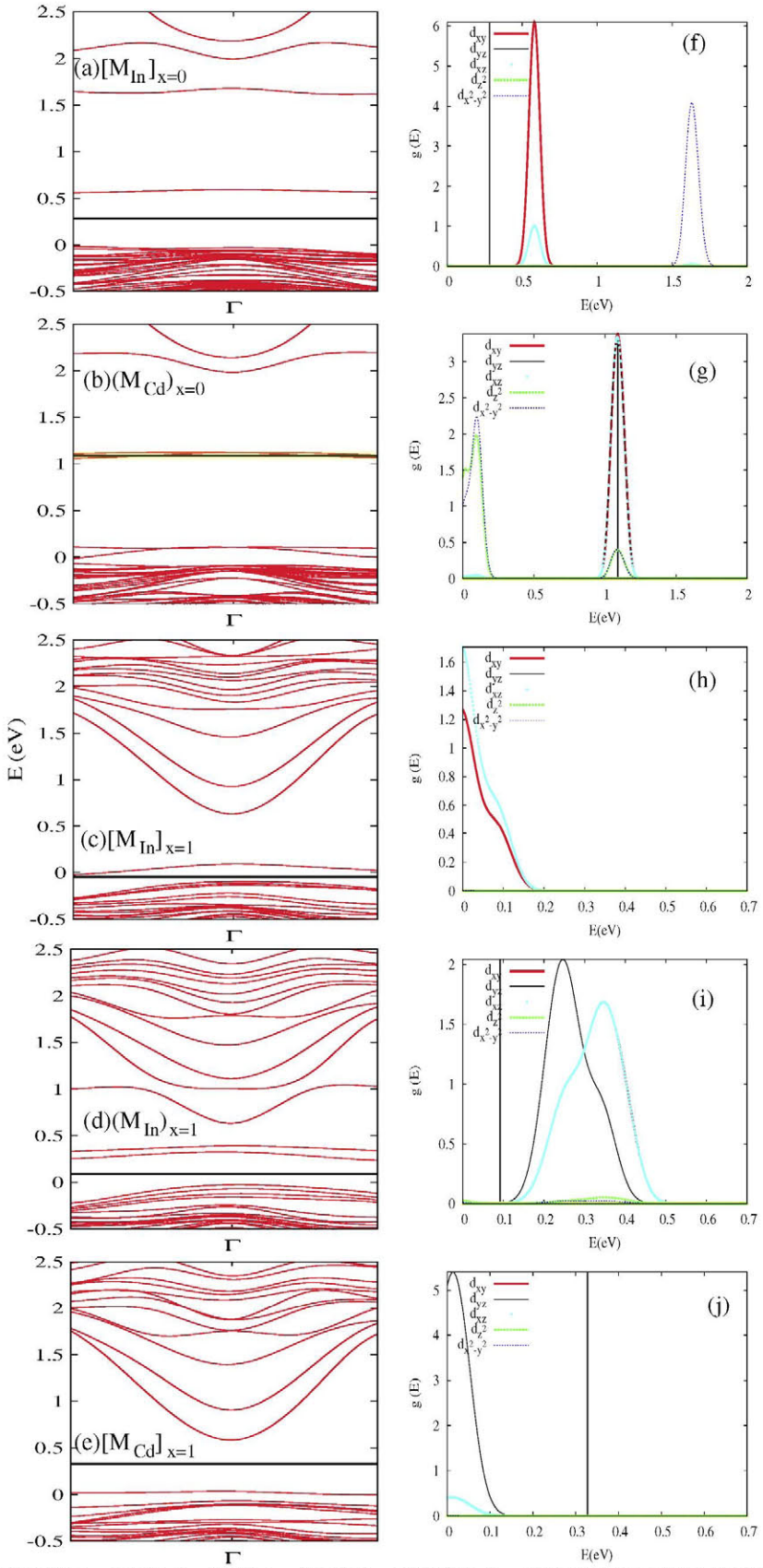


**Fig. 1.** Energy-band diagram for the (a) $[M_{In}]_{x=0}$, (b) $(M_{Cd})_{x=0}$, (c) $[M_{In}]_{x=1}$, (d) $(M_{In})_{x=1}$, and (e) $[M_{Cd}]_{x=1}$ substitutions around the $\Gamma$ point in the BZ with M = V. The square brackets (parenthesis) correspond to the octahedral (tetrahedral) substitution sites. Panels from (f) to (j) represent the projected DOS on the *d*-M orbitals of the panels from (a) to (e) respectively. The VB edge of the $CdIn_2S_4$ host spinel has been chosen as the energy origin. The horizontal (vertical) lines in the panels a–e (f–j) are the Fermi energy for each substitution.

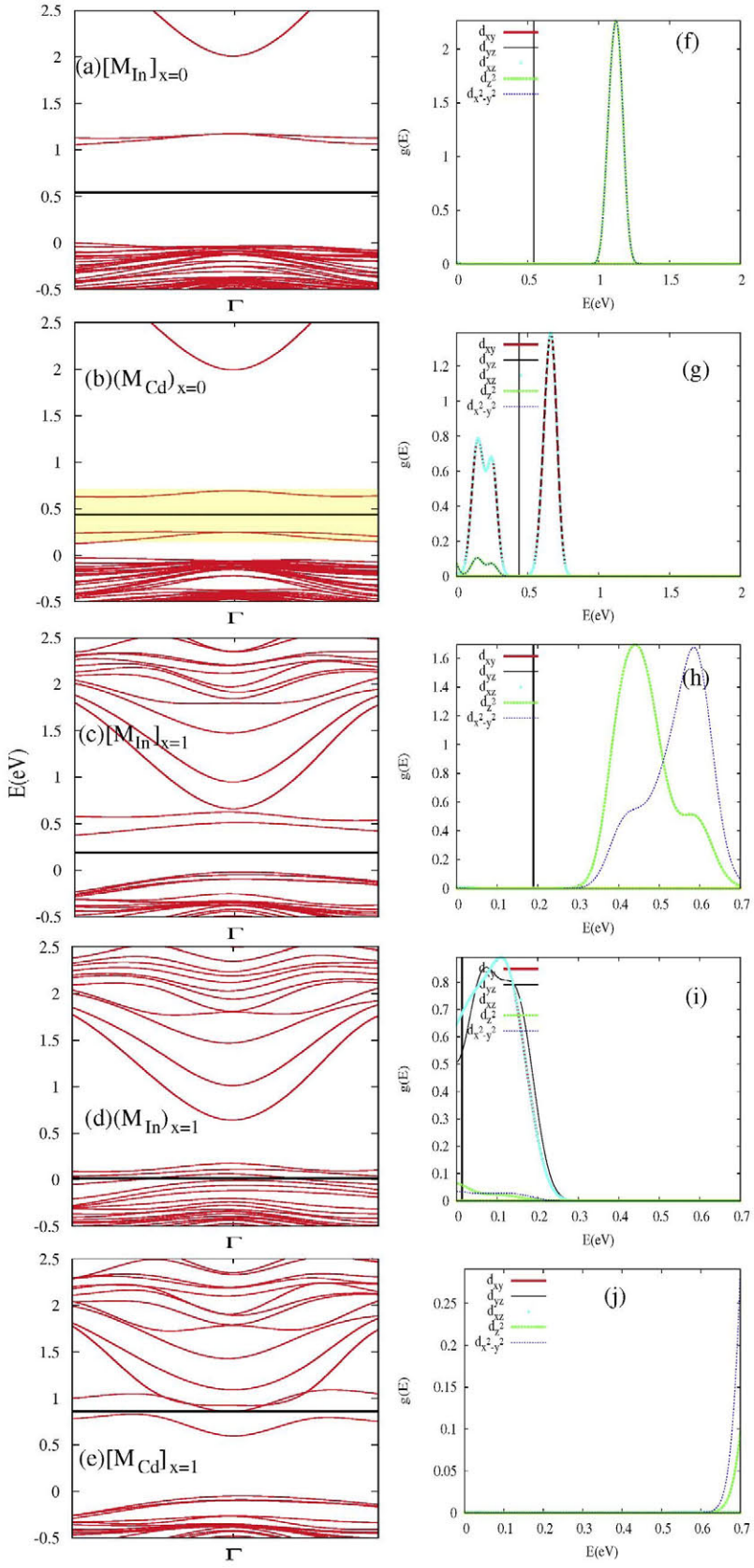


**Fig. 2.** Same legend as in Fig. 1, but for M = Cr.

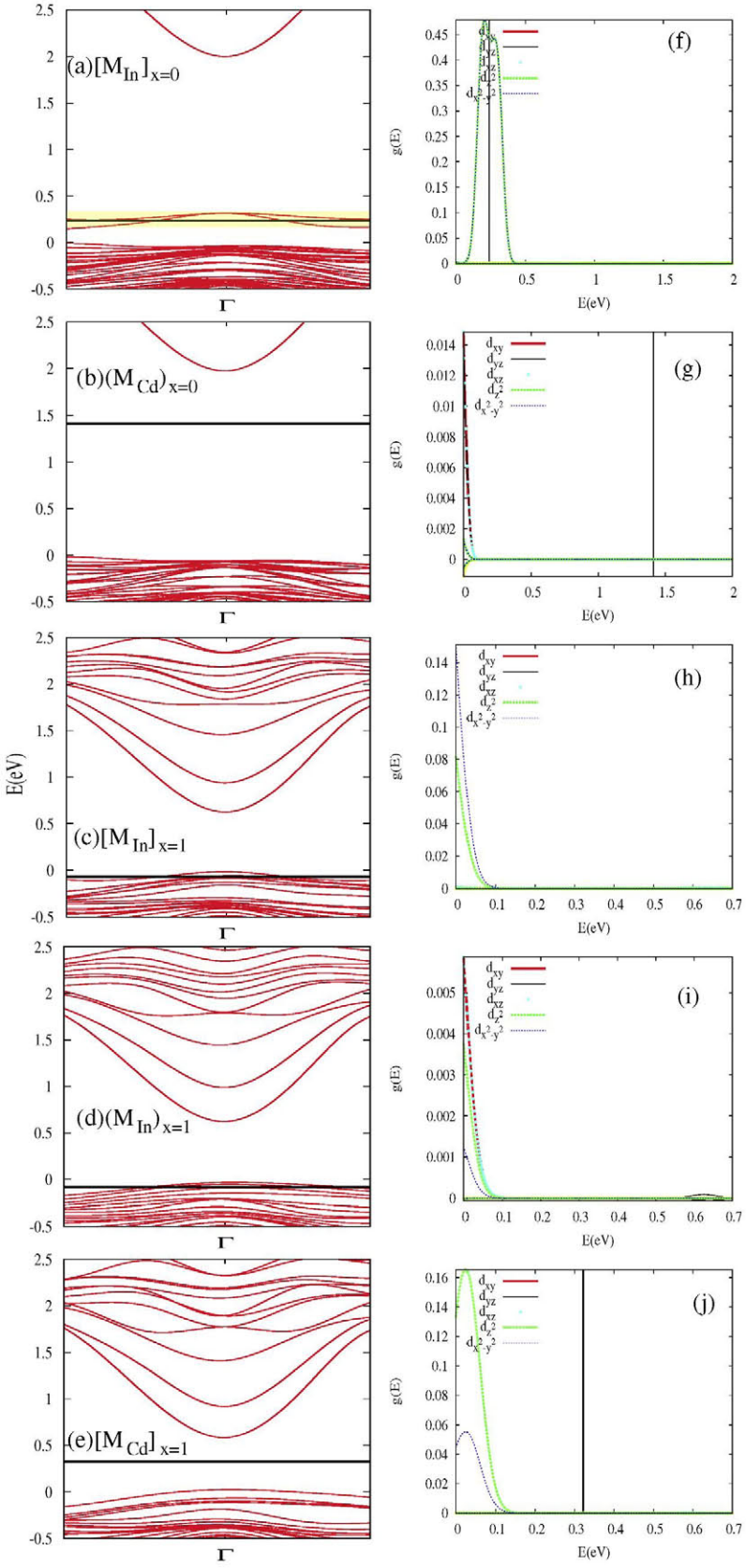


**Fig. 3.** Same legend as in Fig. 1, but for M = Mn.

small distortion is because not all S atoms are symmetrically equivalent.

The substitution energy of Cd by M ($M_{Cd}$ substitution) from the host spinel is estimated as $\Delta E_1 = E[M_yCd_{1-y}In_2S_4] - E[CdIn_2S_4] + y(E_{Cd} - E_M)$, where $E[M_yCd_{1-y}In_2S_4]$ and $E[CdIn_2S_4]$ are the total energies of the spinel with and without the M impurity, $y$ indicates the impurity concentration, and $E_{Cd}$ and $E_M$ are the energies of the elemental atomic reservoirs (isolated Cd and M atoms). This expression is valid for all $M_{Cd}$ sites (octahedral or tetrahedral) substitutions and for any degree of inversion $x$. Of course, the total energy of the host spinel depends on $x$, and the total energy of the substituted spinel depends on both, site and $x$. For the $M_{In}$ substitution, it is only necessary to replace $M_yCd_{1-y}In_2S_4$ and Cd by $CdIn_{2-y}M_yS_4$ and In respectively in the previous equation. This substitution energy may be representative of the relative energy balance expected for the growth processes that use gaseous phases rather than solids for the deposition of the modified compound, like molecular beam epitaxy or physical vapor deposition. The values for the 112-atom supercell ($y = 0.0625$) are represented in Fig. 4a.

For all substitutions $\Delta E_1$ is negative indicating that it is thermodynamically favorable. The most favorable substitutions, in upward order, are for V, Cr and Mn. Its sequence is the descending order of covalent radii. Although the more stable spinel structure is the normal ($x = 0$), when a Cd atom is substituted by the impurity M atom, the substitution energy favors the inverse structure. This is because the initial spinel structure for the substitution is the same as the doped-spinel. The substitution energy depends on the initial spinel structure. But the normal host spinel structure is more stable than the inverse. If the energy of the normal spinel is always used for the initial spinel, then the results of this substitutional energy vary (denoted as $\Delta E_2$ in Fig. 4b): the doped-spinels with normal structure are more stable, except for the $[V_{Cd}]_{x=1}$ substitution, slightly more stable than the substitution in the normal spinel ($([V_{Cd}]_{x=0}$ substitution).

For the $(Cr_{Cd})_{x=0}$, $(V_{Cd})_{x=0}$, and $[Mn_{In}]_{x=0}$ substitutions with a partially-full IB, the transitions VB-IB and IB-CB with lower energy are possible. This can be seen in Fig. 5, which shows the absorption coefficient broken down into the VB-CB, VB-IB, IB-CB and IB-IB transitions for the majority spin component(+). In the single-gap host semiconductor only the VB-CB transition is possible. Thus, these sub-bandgap absorptions increase the mobile carriers

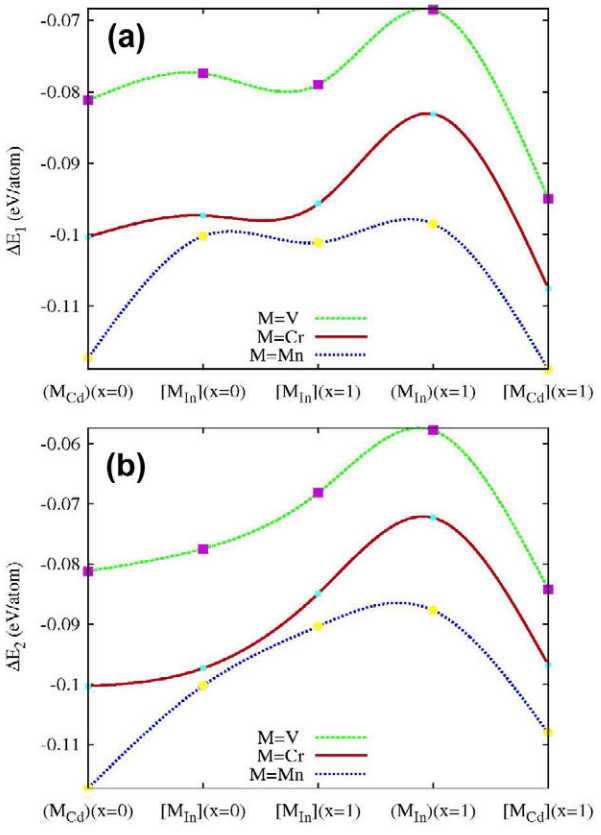


**Fig. 4.** Substitution energy of Cd or In by M from the host spinel. The initial host spinel: (a) has the same structure as the final doped-spinel and (b) has the normal ($x = 0$) structure. Marks indicate the Substitution energy. Lines between marks do not have any meaning. It has been added for as visual effect.

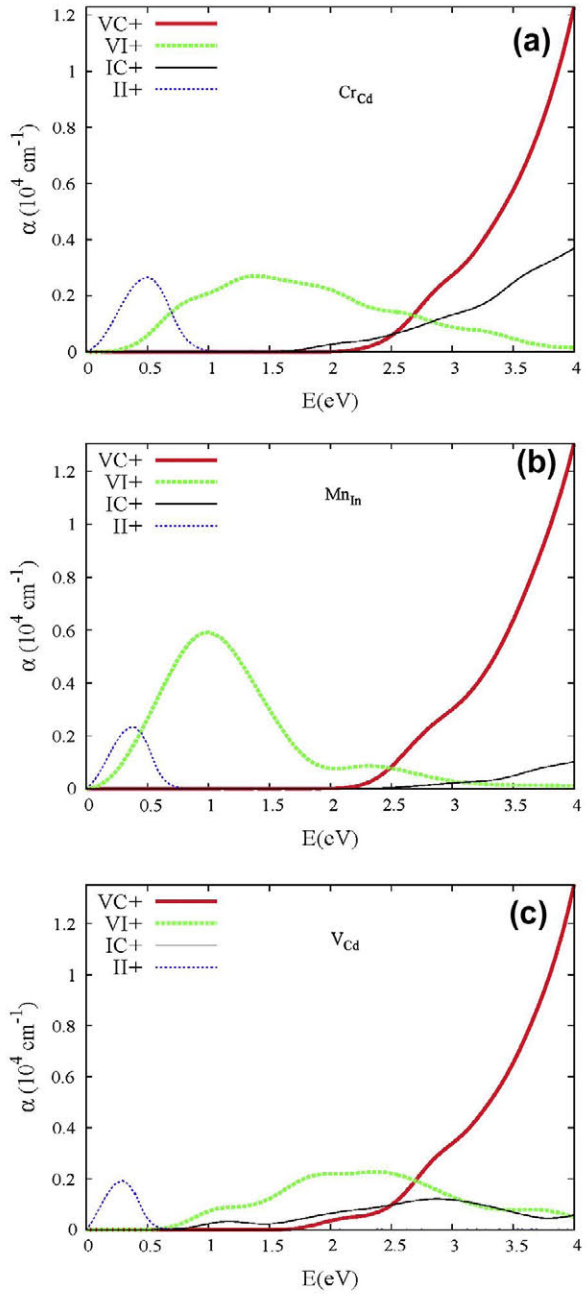


**Fig. 5.** Absorption coefficients $\alpha(E)$ for the majority spin component (+) split in their components: VI+(between VB and IB), VC+(between VB and CB), IC+(between IB and CB), and II+(inside the IB) of the (a) $Cr_{Cd}$, (b) $Mn_{In}$, (c) $V_{Cd}$ substitutions in the normal ($x = 0$) $CdIn_2S_4$ structure.

(electrons in the CB and holes in the VB) with respect to the single-gap host semiconductor. This implies a larger efficiency when these types of compounds are used to absorb the solar radiation in solar cells [10].

## 4. Conclusions

We have presented a theoretical study of the structural and electronic properties of the M-doped ternary spinel semiconductor $CdIn_2S_4$ with M = V, Cr and Mn. All substitutions, in the normal and in the inverse structure, are analyzed for these impurities. The $(Cr_{Cd})_{x=0}$, $(V_{Cd})_{x=0}$, and $[Mn_{In}]_{x=0}$ substitutions present a partially-full IB isolated from the VB and CB. The contribution of the impurity states to these IB are from the $d_t$-states ($d_e$-states) for tetrahedral (octahedral) substitution sites. Most of the possible substitutions are favorable with respect to the host spinel. Nevertheless, the most favorable substitutions are in the normal host spinel. $(Cr_{Cd})_{x=0}$ and $(V_{Cd})_{x=0}$ substitutions are the most favorable substitutions for the Cr and V impurities, whereas the $[Mn_{In}]_{x=0}$ substitution is the second most stable in the normal host spinel for the Mn impurity. Because of the presence of partially-full IB the possibilities of inter-band transitions increase. It could be interesting for applications in optoelectronic devices.

## Acknowledgments

This work has been supported by the National Spanish projects Bibiana (PIB2010US-00096) and the European Commission through the funding of the project NGCPV (FP7-EU-JPN 283798), and by La Comunidad de Madrid through the funding of the project NUMANCIA-2 (Ref. No.: S-2009/ENE-1477).

## References

[1] P. Porta, A. Anichini, U. Bucciarelli, J. Chem. Soc. Faraday Trans. 75 (1978) 1876.
[2] M. Springford, Proc. Phys. Soc. 82 (1963) 1029.
[3] Y. Seki, S. Endo, T. Irie, Jpn. J. Appl. Phys. 19 (1980) 1667.
[4] S.N. Mustafaeva, M.M. Asadov, D.T. Guseinov, Perspekt. Mater. 1 (2010) 45.
[5] H. Nakanish, Jpn. J. Appl. Phys. 19 (1980) 103.
[6] S. Endo, T. Irie, J. Phys. Chem. Solids 37 (1976) 201.
[7] A. Anedda, E. Fortin, J. Phys. Chem. Solids 40 (1979) 653.
[8] S.N. Baek, T.S. Jeong, C.J. Youn, K.J. Hong, J.S. Park, D.C. Shin, Y.T. Yoo, J. Cryst. Growth 262 (2004) 259.
[9] S.I. Radautsan, V.F. Zhitar, I.G. Kosnichan, M.I. Shmiglyuk, Fiz. Tekh. Poluprovodn. 5 (1971) 2240;
S.I. Radautsan, V.F. Zhitar, I.G. Kosnichan, M.I. Shmiglyuk, Sov. Phys. Semicond. (English Transl.) 5 (1971) 1959.
[10] A. Luque, A. Martí, Phys. Rev. Lett. 78 (1997) 5014.
[11] P. Hohenberg, W. Kohn, Phys. Rev. B 136 (1964) 864.
[12] W. Kohn, L.J. Sham, Phys. Rev. 140 (1965) A1133.
[13] J.M. Soler, E. Artacho, J.D. Gale, A. García, J. Junquera, P. Ordejon, D. Sánchez-Portal, J. Phys. Condens. Matter 14 (2002) 2745. and references therein.
[14] J.P. Perdew, K. Burke, M. Ernzerhof, Phys. Rev. Lett. 77 (1996) 3865;
J.P. Perdew, K. Burke, M. Ernzerhof, Phys. Rev. Lett. 78 (1997) 1396.
[15] N. Troullier, J.L. Martins, Phys. Rev. B 43 (1991) 1993.
[16] L. Kleinman, D.M. Bylander, Phys. Rev. Lett. 48 (1982) 1425;
D.M. Bylander, L. Kleinman, Phys. Rev. B 41 (1990) 907.
[17] O.F. Sankey, D.J. Niklewski, Phys. Rev. B 40 (1989) 3979.
[18] H. Hahn, G. Frank, W. Klinger, A.D. Störger, G. Störger, Anorg. Allg. Chem. 279 (1955) 241.
[19] O. Madelung, Semiconductors: Data Handbook, Springer-Verlag, 2000.
[20] S.N. Mustafaeva, M.M. Asadov, D.T. Guseinov, Inorg. Mater. 47 (2011) 844.
[21] W. Czaja, L. Krautsbauer, Phys. Status Solidi 33 (1969) 191;
R. Brown, M.D. Martin, W.A. Shand, J. Phys. C 3 (1970) 1329.
[22] F. Meloni, G. Mula, Phys. Rev. B 2 (1970) 392.
[23] K.Y. Rajpure, V.L. Mathe, C.H. Bhosale, Bull. Mater. Sci. 22 (1999) 927.
[24] H. Nakanishi, S. Endo, T. Irie, J. Phys. Paris, Colloq. 36 (1975) C3–163.
[25] A. Baldereschi, F. Meloni, F. Aymerich, G. Mula, Inst. Phys. Conf. Ser. 35 (1977) 193.
[26] C. Tablero, J. Appl. Phys. 112 (2012) 093108.
[27] C. Tablero, J. Appl. Phys. 108 (2010) 093114;
C. Tablero, Phys. B 404 (2009) 4023.